Environmental Science and Pollution Research (2021) 28:38332–38347
https://doi.org/10.1007/s11356-021-13397-5

RESEARCH ARTICLE

Disruption of brain conductivity and permittivity and neurotransmitters induced by citrate-coated silver nanoparticles in male rats

Azza Attia[1] · Heba Ramadan[2] · Reda ElMazoudy[1,3,4] · Asmaa Abdelnaser[5]

Received: 8 October 2020 / Accepted: 8 March 2021 / Published online: 17 March 2021

Abstract

As one of the most exonerative, competitive, and abundant nanoparticles in curative uses, silver nanoparticles (AgNPs) play a growing important role in developing global neurodegeneration. Herein, we inspected the neurotoxic and histopathological effects of the oral dose of 26.9 nm citrate-coated AgNPs (100 and 1000 mg/kgbw, 28 days) on the brain conductivity and permittivity combined with neurotransmitter assays. While male mice in the control group were given deionized water. In terms of biophysical levels, the brain electric conductivity and relative permittivity were significantly decreased in the 26.9 nm citrate-coated AgNP treated groups versus the controls. Besides, 26.9 nm citrate-coated AgNP treatment resulted in a significant deficiency in the concentrations of brain acetylcholine esterase, dopamine, and serotonin. Total brain contents of silver ion significantly increased in a dose-dependent manner. Further, light and electron microscopy revealed a progressive disruption in the lamellar pattern of the myelinated axons of the nerve fibers, in addition to the accumulation of nanosilver in lysosomes and swollen mitochondria in axoplasm. In conclusion, 26.9 nm citrate-coated AgNPs are capable of gaining access to the brain of mice and causing electric conductivity and relative permittivity damage along with a high degree of cellular toxicity in the brain tissue. Therefore, the present study highlights, for the first time, the adverse effects of the citrate-coated AgNPs to the brain of mice and raises the concern of their probable neurotoxic impacts which is helpful for conclusive interpretation of future behavioral and potential neurodegeneration-based aspects. It would be of interest to investigate citrate-coated AgNPs mediated axonal relevant-signal transduction levels in future studies.

Keywords Nanosilver · Neurotoxicity · Neurotransmitters · Oxidative stress · Conductivity · Permittivity

Azza Attia contributed equally to this work.

Responsible Editor: Mohamed M. Abdel-Daim

✉ Azza Attia
azzaaattia@hotmail.com

✉ Reda ElMazoudy
rhelmazoudy@alexu.edu.eg

[1] Zoology Department, Faculty of Science, Alexandria University, P.O. Box. 21511, Moharram Bek, Alexandria, Egypt

[2] Biophysics Department, Medical Research Institute, Alexandria University, Alexandria, Egypt

[3] Biology Department, College of Science, Imam Abdulrahman Bin Faisal University, P.O. Box. 1982, 31441, Dammam, Saudi Arabia

[4] Basic and Applied Scientific Research Center, Imam Abdulrahman Bin Faisal University, P.O. Box. 1982, 31441, Dammam, Saudi Arabia

[5] Department of Biomedical Sciences, Pharos University, Smouha, Alexandria, Egypt

Introduction

The nanoparticles (NPs, 1 to 100 nm) are ultra-fine materials that have new characters different than that of their bulk forms (Wegner et al. 2006). Therefore, NPs gain new physicochemical and biological properties such as shape, size, distribution, aggregation state, and specific surface areas which give them higher reactivity (Schrand et al. 2010; Azocar et al. 2019).

In recent years, NPs are used in the delivery of drugs, proteins, genes, vaccines, polypeptides, and nucleic acids. Currently, various applications of the drug delivery system via NPs have encountered an enormous position sector like pharmaceutical, medical, and biological (Sahab Uddin and Rashid, 2020; Zahin et al. 2020). However, releasing silver nanoparticles (AgNPs) into the environment from various sources could indirectly affect humans through the food chain (Blaser et al. 2008) and also may cause toxicity to animals

(Tang et al. 2008), plants (Lin and Xing 2007), and bacteria (Choi and Hu 2008). AgNPs may enter the body via the respiratory system, gastrointestinal tract, or through the skin and could not easily be eliminated by physiological clearance systems leading to their accumulation in the tissues and organs (Medina et al. 2007). Also, AgNPs may be capable to penetrate the brain by crossing the blood-brain barrier (BBB) causing the impairment of cell functions and inducing cell damage (Tang and Xiong 2009; Tang et al. 2010). Furthermore, AgNPs may interact with the cerebral microvasculature producing neurotoxicity (Trickler et al. 2010; Grosse et al. 2013). In addition to the degeneration of neuritic processes in vitro (Xu et al. 2013), (Cupaioli et al. 2014) demonstrated that NPs can affect Bax protein levels of mitochondria, causing apoptosis or they can accumulate in the lysosomes impairing their degradation capacity, while Huang et al. (2015) revealed that AgNPs could affect the inflammatory gene expression in neural cells. New researches have demonstrated that dyshomeostasis of essential biometals (calcium, magnesium, manganese, copper, zinc, and iron) is impaired and accumulation of toxic metals is usually observed in numerous neurodegenerative diseases including in the case of Alzheimer's disease. Furthermore, these metals contribute significantly to the metabolism and aggregation of amyloid-beta (Kabir et al. 2021).

Microglia are macrophage-like cells and important mediators of the initial inflammation in the central nervous system that may participate in neurodegenerative diseases, including Alzheimer's and Parkinson's diseases (Ryu et al. 2002). Normally, over a long period, the nanoparticles can accumulate in the neuronal tissues and microglia, causing necrotic degeneration (Tang et al. 2008), and even aggravate the process of brain pathology (Sharma et al. 2010). Eom et al. 2013 and Struzynski et al. (2014) stated that AgNPs could initiate their toxic effects through the production of different types of free radicals. These free radicals and oxidative stress can cause oxidation of lipids, proteins, DNA injury, and apoptosis (Park et al. 2010; Yin et al. 2013a, b). Recent studies have shown that AgNP exposure implements oxidative stress-mediated neurodegeneration including Alzheimer's, Parkinson's, and Huntington's diseases that are characterized by disorders of the structure and/or function of neurons (Sahab Uddin et al., 2020a). Growing evidence suggested that there is an association between neuronal dysfunction and neuroinflammation in Alzheimer's disease, coordinated by the chronic activation of astrocytes and microglial cells along with the subsequent excessive generation of the pro-inflammatory molecule (Sahab Uddin et al., 2020b).

Various studies reported that neural damage is associated with dysfunctions of the neurotransmitter system including acetylcholine esterase (AChE) and dopamine (DA) (Stasiuk et al. 2008). Hussain et al. 2006 found that AgNPs could reduce dopamine concentration, causing many risks to the mammalian brain. Also, Wang et al. (2012) showed that decrease in the dopamine levels associated with the increase in reactive oxygen species (ROS) production by AgNPs.

The dielectric properties of the brain tissue include both conductivity and permittivity that provide important information about cell viability. Changes in the cell membrane permeability are associated with the change in the membrane conductance, all leading to cell death. Baruwati et al. (2013) demonstrated that exposure to the green synthesized AgNPs could alter the membrane permeability and stimulate oxidative stress pathways in neurons.

Histologically, Genter et al. (2012) assessed the distribution and toxic potential of AgNPs following intranasal exposure, and it was found that these particles accumulated in the lateral brain ventricles. Several studies have also shown that AgNPs deposit in the brain after exposure via different routes and cause certain types of brain damage (Xu et al., 2015).

As being highly toxic, toxicological effect of AgNP exposure is an important issue concerned by many researchers, and has been tested in various aspects. Of them, Alzheimer's disease is a chronic neurodegenerative disorder that is marked by cognitive dysfunctions and existence of neuropathological hallmarks such as amyloid plaques and neurofibrillary tangles (Sahab Uddin et al., 2021).

Accordingly, in the present study, we maintained male rats under different citrate-coated AgNP-26.9-nm concentrations throughout 28 days of the experimental period and then measured the brain electrical conductivity and brain dielectric permittivity, neurobiochemical parameters, and antioxidant stress responses of rats to assess the combined neurotoxic effect of AgNPs. Especially, we aimed to test whether chronic neurotoxicity of AgNPs on male rats would be enhanced more under brain electrical conductivity and dielectric permittivity milieu along with histological and ultrastructural alterations. Besides, the present study might provide an additional contribution to neurotoxicological aspects of potential impacts of AgNPs pollution.

Materials and methods

Sampling collection, preparation, and preservation

a. Synthesis of citrate-coated silver nanoparticles

Silver nanoparticles were prepared in the Biophysics Department, Medical Research Institute, Alexandria University, Alexandria, Egypt. The particles were processed according to the chemical reduction method of (Pal et al. 2007) based on the reduction of silver nitrate ($AgNO_3$) with sodium citrate.

b. Lyophilization of citrate-coated silver nanoparticles

Citrate-coated silver nanoparticles were frozen by vacuum freeze-drying machine work at 230 V, 50 Hz. The obtained solutions were placed in falcon tubes, frozen in liquid nitrogen, and freeze-dried by vacuum freeze drying/lyophilization equipment (LyoCapsule Freeze Dryer™, SP Scientific, New York, USA) at a pressure of 26.5 Pa and 5% saccharine which was used as cytoprotectant.

c. Characterization of citrate-coated silver nanoparticles

i. UV-VIS spectral analysis

The bio-reduction of pure Ag^+ ions in aqueous solution was detected by a sampling of aliquots (0.2 ml) of the colloidal suspension, then diluting the samples with 2 ml deionized water and subsequently measuring UV-VIS spectra of the resulting diluents using UV/VIS Spectrophotometer (Germany). The maximum absorption was scanned at the wavelength of 300 - 800 nm.

ii. Transmission electron microscope analysis

Transmission electron microscope (TEM) analysis was employed to visualize the size and shape of AgNPs. A drop of aqueous suspension (50 μl) containing the biosynthesized AgNPs was placed on the carbon-coated copper grids after allowing the water to evaporate, drying in air. TEM micrographs were taken by analyzing the prepared grids on a JEOL TEM instrument.

iii. Particle size analysis

The particle size distribution of the AgNPs was determined by laser light scattering on a Beckman Coulter Particle Size Analyzer (N5 submicron particle size analyzer, Japan). The AgNPs were added to the sample dispersion unit containing the stirrer and stirred to reduce the aggregation between them. The mean particle size was measured after experimenting triplicate.

iv. Particle agglomeration analysis

Characterization of nanoparticle agglomeration in the deionized distilled water was conducted using a Zetasizer instrument (Nano-ZS, 4 mW He–Ne 633 nm laser).

Animals and experimental approval

Forty-five adult male CD-1 mice (3 months old, weighing 28–32 g) were obtained from the animal house of Medical Research Institute, Alexandria University, Alexandria, Egypt. The males acclimatized for 2 weeks (5 mice/stainless steel cage) at 25 ± 2 °C room temperature, 55 ± 5% humidity, and normal photoperiod day/night. The animals were allowed free access to food and drinking water ad libitum throughout the study.

AgNPs treatment dose

Synthesized prepared citrate-coated AgNPs were orally administered at a concentration of 100 and 1000 mg/kgbw for experimental groups AgNPI and AgNPII, respectively (28 days, 15 mice/each). In the control group, mice have received deionized water. The dose levels were selected based on the LD50 of previous studies (5000 mg/kg) on 28-day oral administration of silver nanoparticle (100 and 1000 mg/kgbw equivalent to 1/50 and 1/5 mg/kgbw, respectively) (Maneewattanapinyo et al. 2011; Adeyemi and Adewumi 2014).

Brain tissue handling techniques

On reaching the empirically determined endpoint, animals were euthanized by intraperitoneally injected ketamine 80 mg/kg and xylazine 10 mg/kg followed by decapitation. The whole brains (controls and treated) were rapidly excised removed and sectioned along sagittal midline into two halves. The right cerebral hemisphere was fixed for microscopical methods. The whole left half was reserved in liquid nitrogen and frozen at − 80 °C for neurochemistry assay.

Total nanosilver content in the brain

The total silver content in the whole brains after 28 days of treatment was quantified measured determined by using an inductively coupled plasma-atomic emission spectrometer (R-R-smz-ICPE-9820 Simultaneous ICP, SHIMADZU EUROPA GmbH, Duisburg F. R. Germany) (Pröfrock and Prange 2012). Data are shown as the average of four independent values.

Energy-dispersive X-ray (EDX) analysis

Identification of the elemental composition of the brain tissues was generated by energy-dispersive X-ray analysis (EDX). It consists of spectra showing peaks corresponding to the elements making up the true composition of the brain samples.

Brain tissue homogenization

AgNP-treated male mice and controls (three experimental replicates per group) were sacrificed after 28 days by decapitation and dissected. The brains were rapidly excised removed, washed in cold buffered phosphate (pH 7.4) and homogenized (Rotary homogenizer BK-HG160, Biobase, China). The homogenized brain tissues were centrifuged at 1600 rpm for

20 min at 5 °C, and the supernatant was immediately stored at −40 °C for further neurochemical assessment.

Neurochemistry methods

a. Brain acetylcholine esterase assay

Acetylcholine esterase (AChE, Acetylcholine esterase Assay Kit, Colorimetric, Catalog No. STA-603) activity was assayed in triplicate using the technique of the colorimetric procedure of Ellman et al. (1961). The cholinesterase activities were accomplished at absorbance 670 nm.

b. Brain dopamine assay

Quantitatively, dopamine in brain supernatants was measured by a competitive ELISA assay following Bio Vision's Dopamine ELISA kit (Catalog No. K4219-100) protocol. The average of the triplicate readings for samples was at 450 nm, detection range 1.56–100 ng/ml, and sensitivity <0.938 ng/ml (Anton and Sayre 1964).

c. Plasma and brain serotonin assay

In the next morning of the last AgNP intake and fasting overnight, venous blood was gathered from the vena cava by using the catheter in 9-ml ACD-A Vacuette® tubes (Cat. No. 455055, Greiner Bio-One International GmbH, Germany). Following instructions of the manufacturer, competitive enzyme immunoassay (commercial ELISA Kit, ab133053) was used for colorimetric detection of serotonin contents in brain supernatants and concentration of serotonin in plasma (triplicate) (Lee et al. 2014).

Biophysical analysis

Brain electrical conductivity (σ) and brain dielectric permittivity (ε)

One centimeter of the brain tissue from control and the experimental-treated mice was used for dielectric measurements. Capacitance and resistance of the brain tissue were measured using LCR meter (L for inductance, C for capacitance, and R for resistance). This LCR meter operates at a frequency range from 1 to 100 kHz with an accuracy of 0.05%. The relative dielectric permittivity ε' and real conductivity σ are calculated according to the following equations:

$$C = \varepsilon' \varepsilon_0 \, A/d \quad (1)$$

$$G = \sigma \, A \, / \, d \quad (2)$$

where C is the capacitance in Farad, G is the conductance in Siemens, of the capacitor between the two measuring electrodes, A is the surface area of the electrode in a square meter, d is the separation between the two electrodes in meter, ε: the relative permittivity (Farad/meter), ε_0: the permittivity of vacuum (8.85×10^{-12}F/m), and σ the electrical conductivity (Siemens/m).

Estimation of brain total antioxidant capacity

By deproteination procedure of 0.1 ml of supernatant by 2 ml of methyl alcohol, vortexed, and centrifuged (30 s, 10,000 r/min/10 min), 1.5 ml methanol and 0.5 ml of DPPH solution were mixed thoroughly with supernatant (colorimetric Kit ab65329). Absorbance at 570 nm was recorded as nanomoles of blank referenced ascorbic acid (Koracevic et al. 2001).

Microscopical methods

a. Light microscopy

The right cerebral hemispheres of the brain tissues were cut into 5-mm specimens and fixed in a 10% neutral buffered formalin, dehydrated, cleared by xylem, and embedded in paraffin wax (Bancroft and Gamble 2008). Thereafter, 5-μm coronal sections were stained with hematoxylin and eosin.

b. Transmission electron microscopy

One-square millimeter specimens of the right cerebral hemispheres of both control and the experimental mice were immediately transferred to a fixative mixture of 4% paraformaldehyde, 1% glutaraldehyde, and phosphate buffer (0.1 M, pH 7.4) at 4 °C for 24 h. The specimens then were post-fixated using 1% buffered Osmium tetroxide (OsO4) at 4 °C for 2 h. Thereafter, the samples were washed several times with phosphate buffer for 30 min, dehydrated through a combination of ascending grades of ethanol with propylene oxide, and finally blocked in a mixture of 1:1 of Epoxy-Araldite resin mixture. Sixty-nanometer ultrathin sections were obtained with a glass knife on LKB ultramicrotome, mounted on 200 mesh naked copper grids, and subsequently double stained with uranyl acetate and lead citrate for 20–30 min, examined at Joel TEM (Robards and Wilson 1993).

Statistical analysis

Statistical analyses were performed using PASW Statistics 18. Normality test was performed using Kolmogorov-Smirnov test, and independent T-test was used to compare the means of each of the two different studied groups when data were normally distributed, while the Mann-Whitney test was performed to compare the medians of each of the two different studied groups when data were not normally distributed.

Results

Characterization of silver nanoparticles

The results of particle size analyzer for citrate-coated AgNPs showed that more than 90% of the prepared particles are in the average size of 26.9 nm, and about 10% of the particles are oversized with baseline error of 1.35% (Fig. 1A). Examination by the transmission electron microscope revealed that most of the citrate-coated AgNPs are spherical, having smooth and homogeneous surfaces. Analysis of the characteristic state of dispersion of AgNPs using dynamic light scattering showed a low level of agglomeration or adhesion and a high level of uniformity. Further, the polydispersity of most of AgNPs particles is 0.74 (i.e., less than 1), indicating the homogeneous distribution with >90% uniformity in size of the particles (Fig. 1B). UV-visible spectrum analysis showed that the maximum absorption wavelength for the particles is at 422 nm (Fig. 1C).

Total silver ion content in brain tissue

The results of total brain ion contents of silver revealed a significant increase in a dose-dependent manner being 0.611 ± 0.017 μg/g and 0.851 ± 0.036 μg/g for 100 mg/kg and 1000 mg/kg (AgNPI and AgNPII groups), respectively, compared with the control group (0.206 ± 0.011 μg/g).

Elemental composition of brain

The energy-dispersive X-ray analysis of the brain tissues of both control and the treated mice revealed the presence of

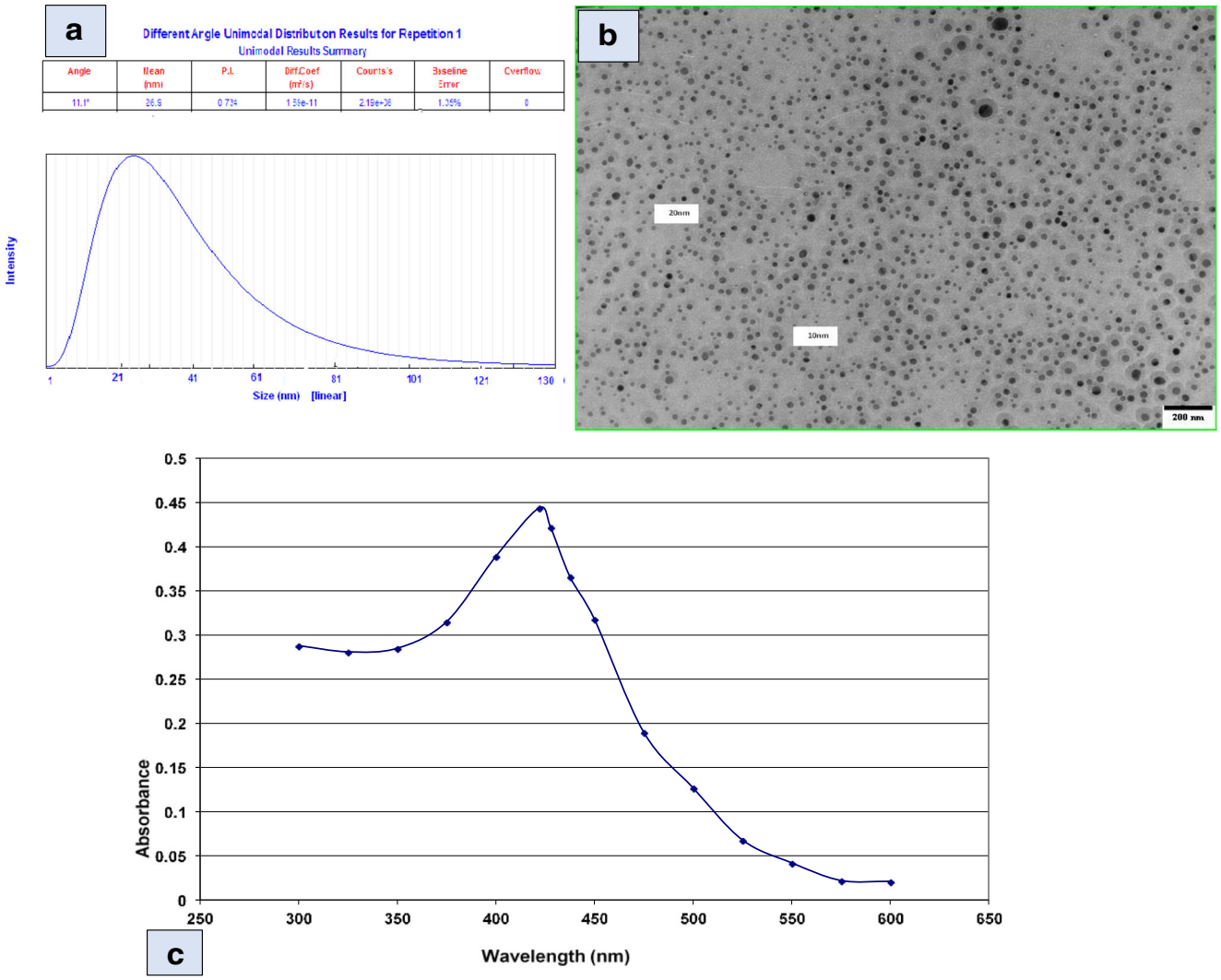

Fig. 1 Characterization data for silver nanoparticles. (A) 90% of the AgNPs show mean particle size of 26.9 nm. The polydispersity of most of AgNPs is 0.74. (B) TEM shows most of the AgNPs are spherical in shape with smooth and homogeneous surfaces and showed a low level of agglomeration with high level of uniformity. (C) UV-visible spectrum analysis shows the maximum absorption wavelength for the particles is at λ max = 422 nm

many different elements including silver (Ag). These elements are phosphorus (P), sulfur (S), potassium (K), calcium (Ca), sodium (Na), copper (Cu), aluminum (Al), and zinc (Zn). However, considerable high levels and high spectral peaks of silver were recorded in the brain tissues of mice administered with 1000 mg/kgbw of AgNPs, compared with those treated with 100 mg/kgbw, indicating silver accumulation in the brain. No observed silver was detected in the brain of the control mice (Fig. 2).

Total antioxidant capacity

From the analyzed data of Fig. 3, it clearly showed that Ag-26.9 nm significantly decreases the antioxidant capacity of the brain in a dose-dependent manner. The decreased antioxidant capacity was more statistically significant in the dose of 1000 mg/kgbw than the dose of 100 mg/kgbw of silver nanoparticles versus controls.

Dopamine levels

The oral administration of silver nanoparticles significantly decreases the levels of dopamine by 58.1% when the mice of the 1000-mg/kgbw group were compared with the control mice. While in mice of the 100-mg/kgbw group, the impacts of the silver nano on dopamine levels significantly minimize by 26.4% compared with the controls (Fig. 4A).

Acetylcholine esterase activity

A significant decrease was observed in the mean value of the enzyme activity of acetylcholine esterase in the mice of the AgNPI and AgNPII groups compared to the controls. Notably, the level of acetylcholine enzyme activity was dose-dependent. Moreover, the highest decrease was observed in the 1000-mg/kgbw group (Fig. 4A).

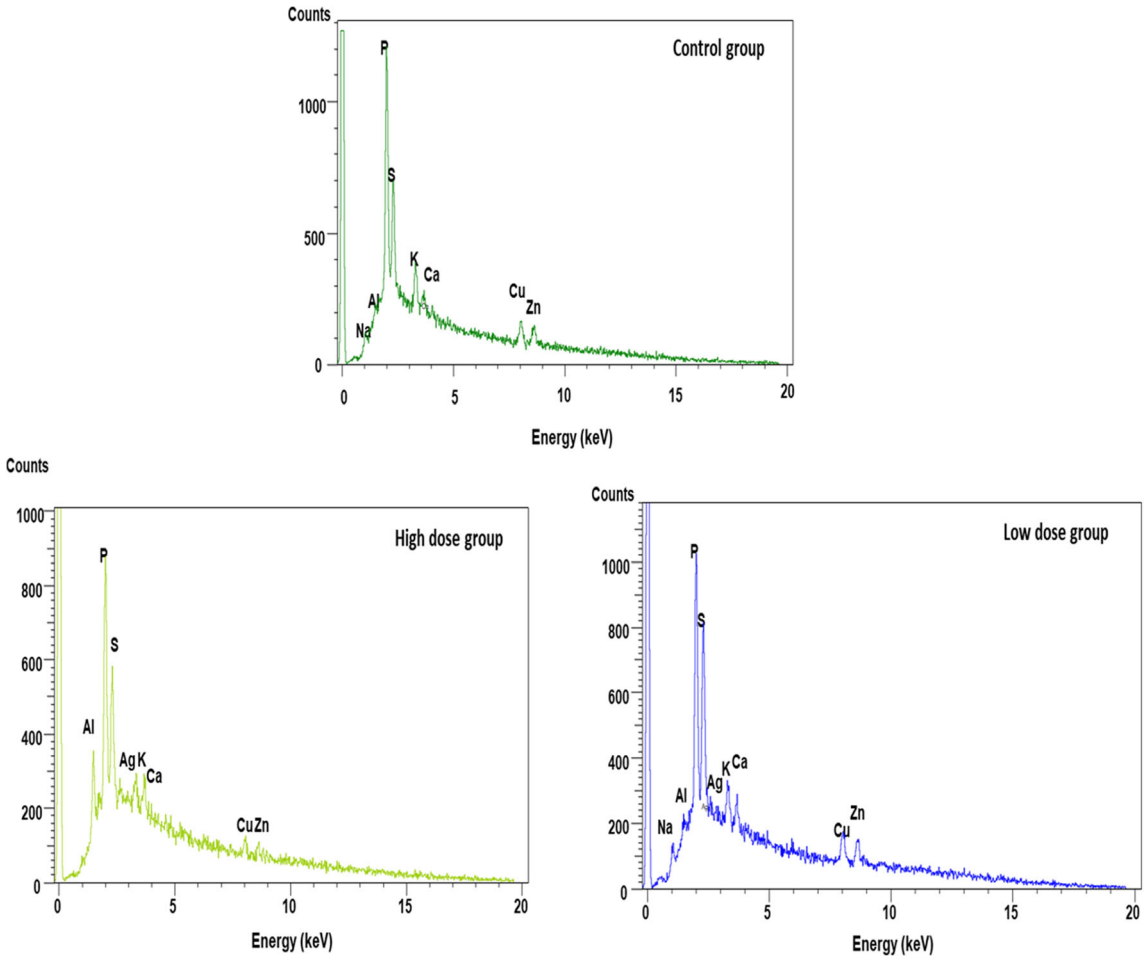

Fig. 2 Energy-dispersive X-ray (EDX) analysis of the brain tissues of control, low dose (AgNP I, 100 mg/kgbw), and high dose (AgNP II, 1000 mg/kgbw) AgNP-treated mice for 28 days

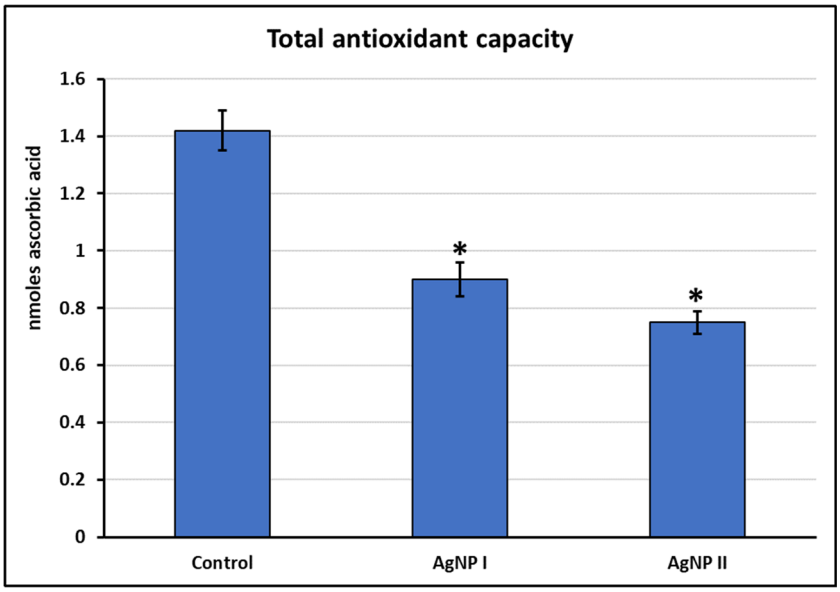

Fig. 3 Effect of 26.9-nm AgNPs on total antioxidant capacity in mice brain tissues of control and treated for 28 days. Data represent means ± SD (n = 15 mice, triplicate). *Significant at $P \leq 0.05$ versus control. Control; AgNP I: 100 mg/kg silver nanoparticles; AgNP II: 1000 mg/kg silver nanoparticles

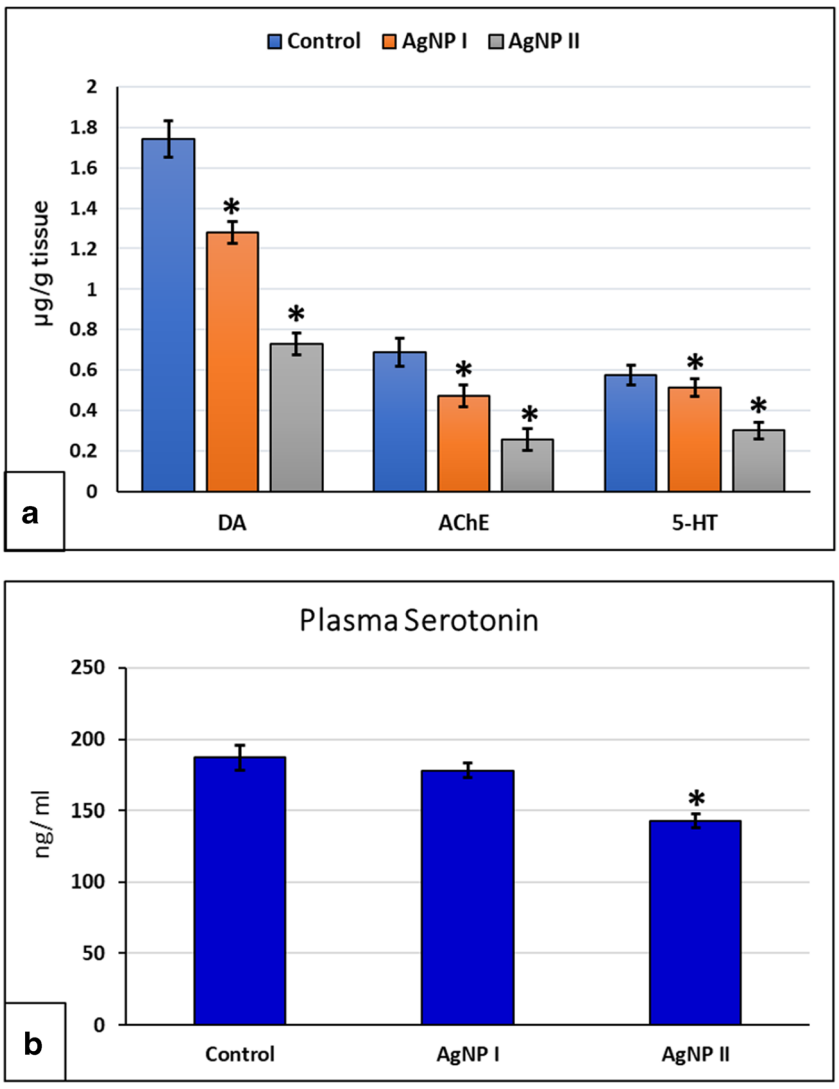

Fig. 4 Effects of 28-day oral administration of 26.9-nm silver nanoparticles (Ag-26.9). (A) The contents of brain monoamines (DA and 5-HT) and AChE activity in cerebral cortex of controls and treated mice. (B) Levels of the plasma 5-HT. Data are expressed as the mean ± SD (n = 15, triplicate). *$P \leq 0.05$ versus the control group using Tukey's post hoc test. DA, dopamine; 5-HT, serotonin; AChE, acetylcholine esterase. Control; AgNP I: 100 mg/kg silver nanoparticles; AgNP II: 1000 mg/kg silver nanoparticles

Plasma and brain serotonin levels

In both brain (Fig. 4A) and plasma (Fig. 4B), the levels of serotonin (5-HT) showed a significant decrease in 100 mg/kgbw and 1000 mg/kgbw of silver groups (AgNPI and AgNPII) compared to controls. This decrease being significantly higher by 1000 mg/kgbw (AgNPII) dose than that by 100 mg/kgbw (AgNPI) (Fig. 4A, B).

Brain conductivity (σ) and brain permittivity (ε)

The biophysical findings revealed that the brain conductivity was gradually decreased (dose-dependent) with increasing the frequency of the applied electric field in the brain tissues of mice administered with the two concentrations (100 and 1000 mg/kgbw) of Ag-26.9 nm. This decrease was parallel with the decrease in the relative permittivity that shown to be decreased suddenly and then started to be saturated (Fig. 5A, B).

Brain histopathology

a. Light microscopic observations

The cerebral cortex of mice treated with 100 mg/kgbw of AgNP-26.9 nm showed neuron pyknosis and observable increase of the neuroglia cells (gliosis) located within the moderately vacuolated neuropil (neuropils spongiosis) (Fig. 6B, C) comparable to control brain tissue (Fig. 6A). However, sections of the cerebral cortex of mice treated with 1000 mg/kgbw Ag-26.9 nm showing the focal area of hemorrhage and the neurons appeared shrunken, containing pyknotic nuclei. Besides, many swelling and hypertrophied neuroglia cells could be found in the injured area of the neuropil spongiosis (Fig. 6D, E).

b. Electron microscopic observations

Using the electron microscope, the neurons in the cerebral cortex of the control mice have large centrally located

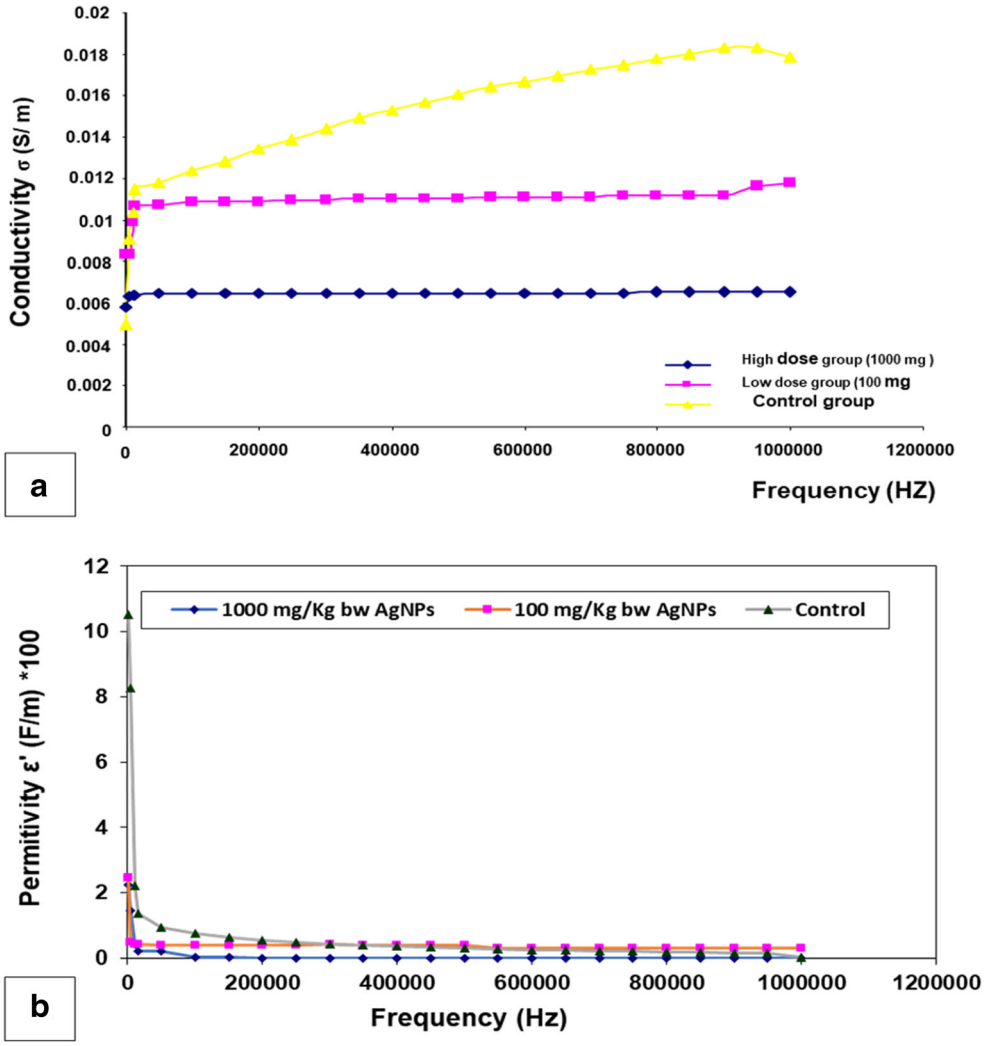

Fig. 5 Biophysical analysis. (A) Variation of the relative permittivity ε' (F/m) with frequency F (Hz). (B) Variation of the real conductivity σ' (S/m) with frequency (Hz). Control; AgNP I: 100 mg/kg silver nanoparticles; AgNP II: 1000 mg/kg silver nanoparticles

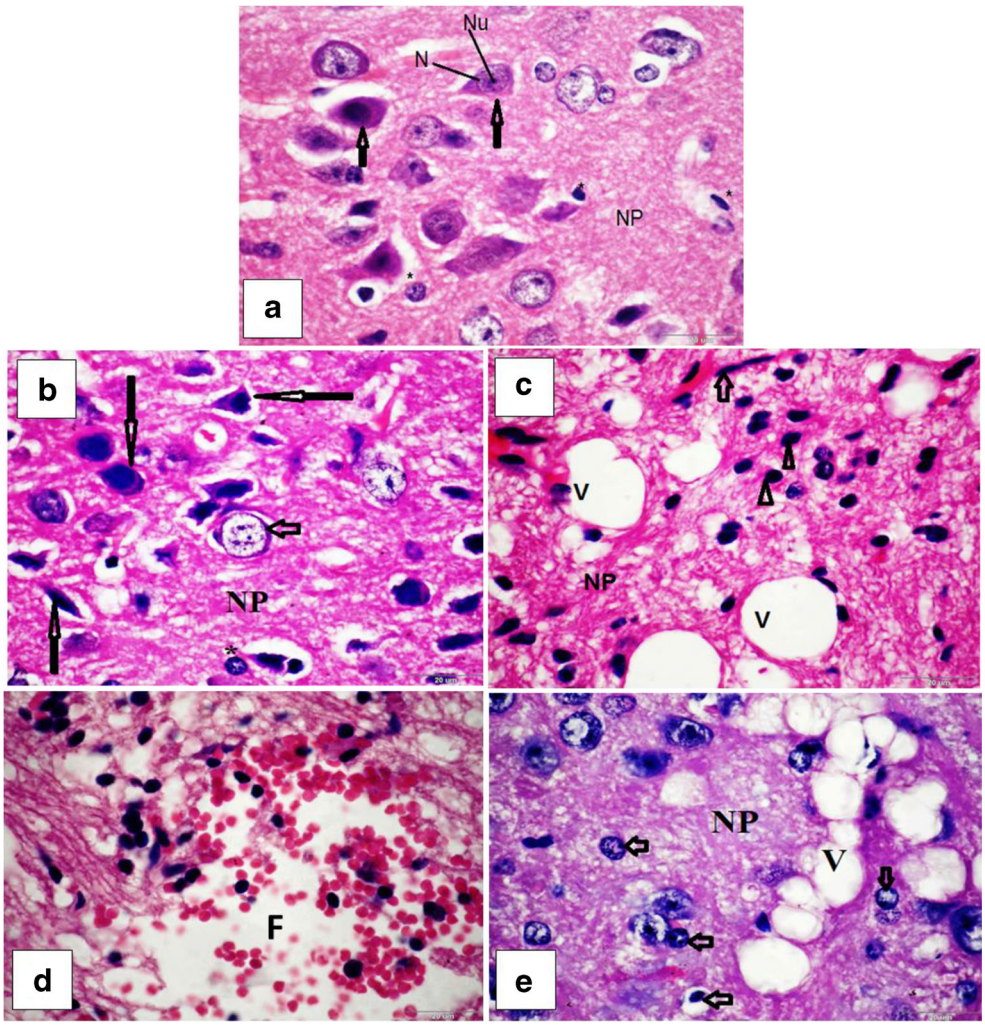

Fig. 6 Photomicrographs of the cerebral cortex sections in control and experimental groups. (A) Control group showing normal configurations of the neuronal tissue. (B) and (C) 100 mg/kg group. (D) and (E) 1000 mg/kg group. Notice: the pyramidal-shape neurons with large nuclei (N, short arrow); pyknotic nuclei of neurons (long arrows); area of gliosis (arrowheads); focal area of hemorrhage (F); vacuolation in the neuropil (spongiosis) (NP); vacuolation (V). H&E

indented nuclei and containing prominent nucleoli (Fig. 7a). The cytoplasm contains numerous free ribosomes and there was a well-developed Golgi saccule adjacent to the nucleus (Fig. 7a). The myelinated axons of nerve cells were distributed in the normal area of neuropil (Fig. 7b). The neuropil contains axon terminals with their large vesicles, mitochondria, and synapses (Fig. 7c).

The electron micrographs of the cerebral cortex of mice administered with 100 mg/kgbw AgNPs revealed moderate ultrastructural alterations including neuronal shrinkage, an indentation in the nuclear envelope, in addition to the enlargement of the nucleolar size (Fig. 8a). The myelin sheath showed an observable decrease and multiple splitting (separation) of their myelin lamellae with wide spaces in between. The area of neuropil was finely vacuolated because of swelling of the neuronal processes and synapses (Fig. 8b). The synaptic vesicles have well-defined structures, and the vesicles were arranged in the cluster as in the control (Fig. 8c). The electron micrographs of neurons of the cerebral cortex of mice treated with 1000 mg/kgbw AgNPs showed marked irregularities in their nuclear envelope. Small dark nanosilver deposits were observed in the nucleoplasm of neuronal cells, in the blood capillaries, and in many lysosomes (Fig. 9a). Moreover, a myelin-like body (myelin figure) contained remnants of synaptic vesicles or disturbed mitochondria were observed, and it represents the initial stage of macroautophagosomes (Fig. 9b). In the area of neuropil, severe degenerative changes were seen in the myelinated axons. This was in the form of defective, disruption, irregular myelination, splitting, and loss of lamellar structure around the nerve fibers. The axoplasm contains swollen irregular mitochondria with destroyed cristae. Moreover, the results revealed local swelling in synapses, and aggregation of the free synaptic vesicles, which were loosely located in the neuropil and were not surrounded by the presynaptic membrane (Fig. 9c).

Discussion

The present assays infer that oral gavage with 26.9 nm citrate-coated AgNPs was absorbed, distributed, and then eventually traversed the blood-brain barrier in vivo inducing

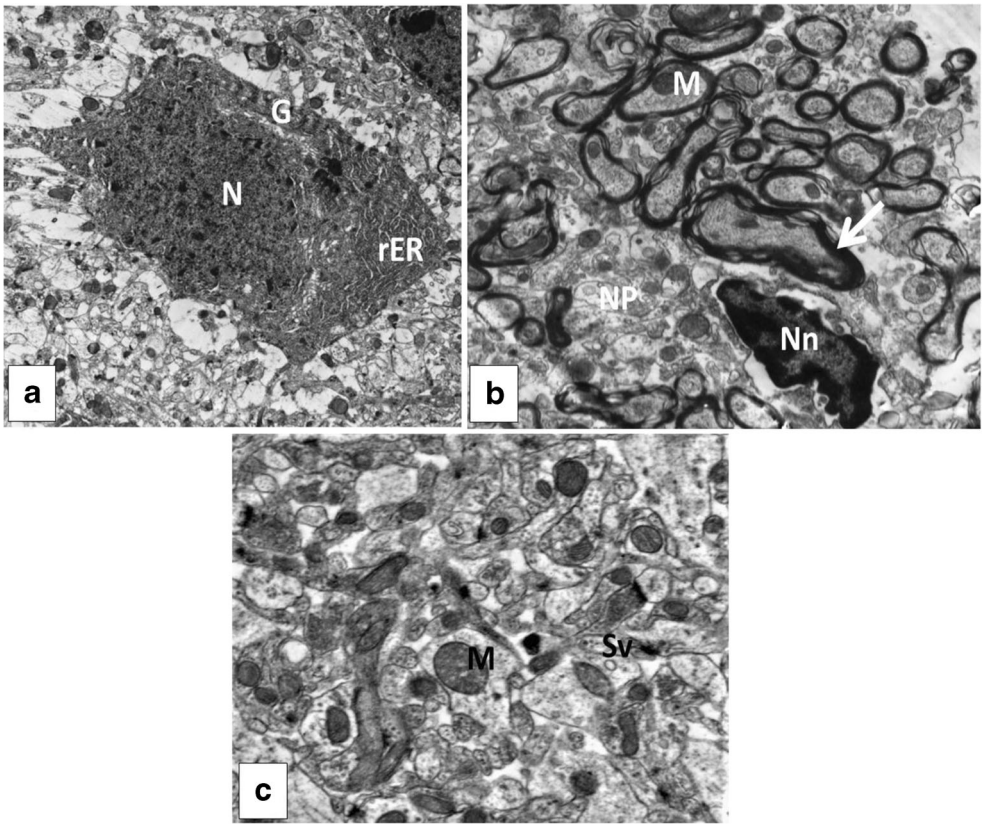

Fig. 7 Electron micrographs of section of cerebral cortex of control mice. (a) Nucleus (N) of neuron; (b) the myelinated axons of nerve fibers (arrows), neuropil (NP), mitochondria (M), nucleus of a neuroglia (Nn); (c) area of neuropile containing processes of nerve fibers, the axoplasm contains rounded mitochondria (M) proper distribution of synaptic vesicles (Vs). × 3000

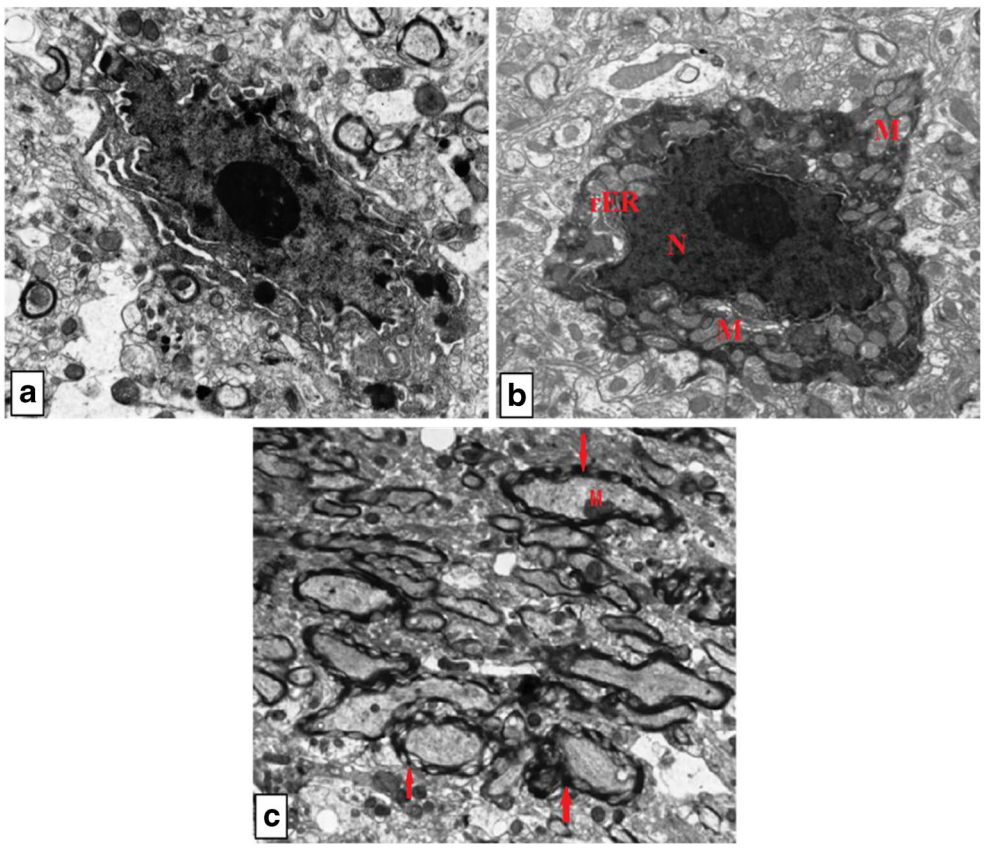

Fig. 8 Electron micrographs of sections of cerebral cortex of mice treated with 100 mg/kgbw AgNPs. (a) Indentation in nucleus of neuron (arrow); neuropil area (NP). (b) Nucleolus (Nu); mitochondria (M); (c) myelin showed an observable decrease and multiple splitting (separation) of their myelin lamellae with wide spaces in between (arrows). × 3000

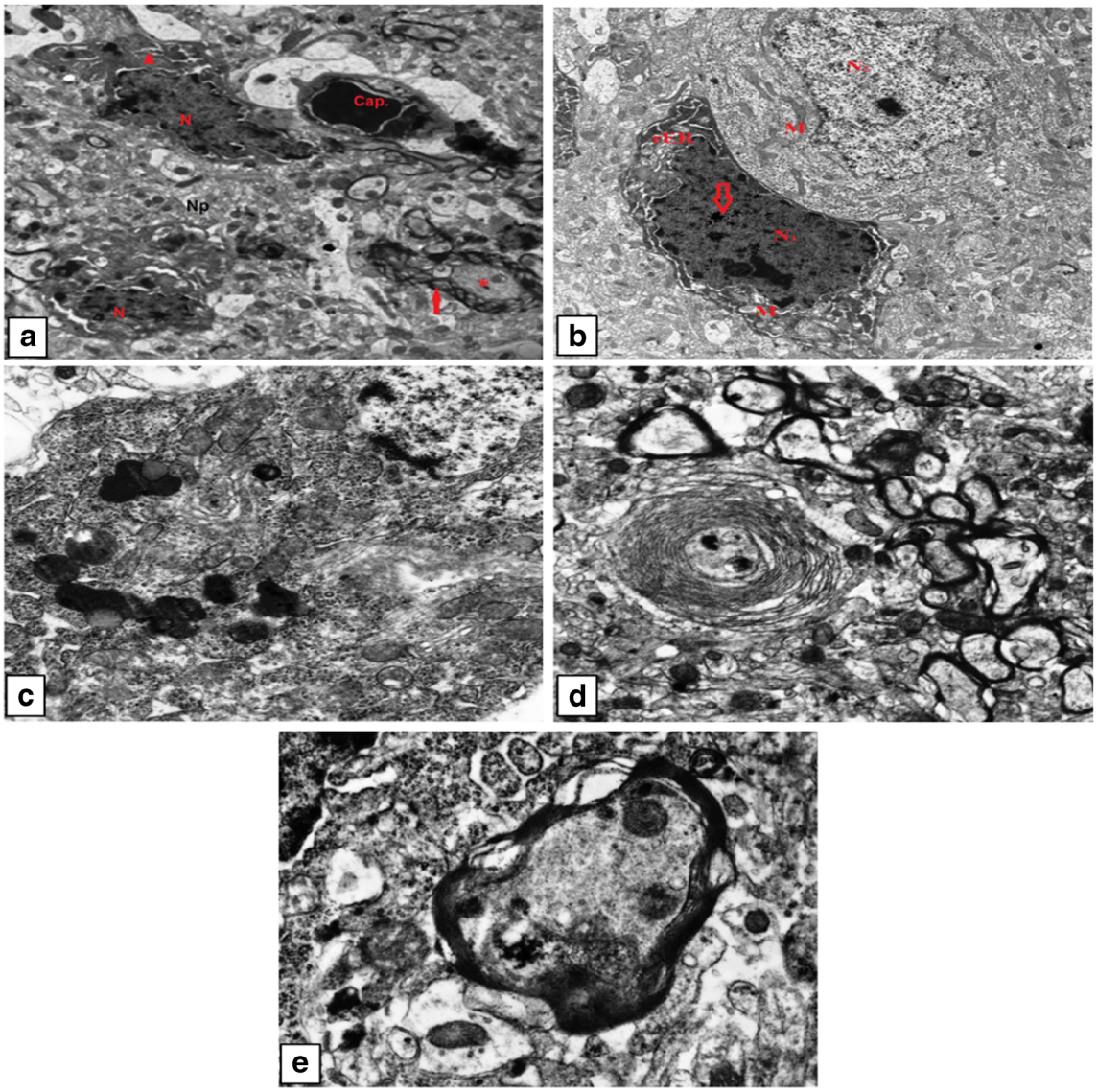

Fig. 9 Electron micrographs of sections of cerebral cortex of mice treated with 1000 mg/kgbw AgNPs, showing: (a) marked irregularities in the nuclear envelope (arrowhead) of the neuronal nucleus (N); the blood capillary (Cap) contains small dark nanosilver deposits; (b) chromatolysis (arrow); dilatation of rER; (c) nanosilver deposits in lysosomes (S); hypertrophied mitochondria (M); (d) the axoplasm contains swollen mitochondria (M); (e) loss of lamellar structure of the myelinated axons (arrow); deposition of the nanosilver granules (S). × 3000

neurotoxicity. Exposure mode (ingestion, intranasal, intraperitoneal) and particle size together with characteristics of surface charge activity, hydrophilicity, and lipophilicity are substantial factors contributing to the toxicity of nanomaterials (Liu et al. 2012; Wang et al. 2015; Wen et al. 2016; Islam et al. 2017; Iqbal et al. 2018). Besides, the physicochemical characteristic is a bioactive agent that can reinforce the ability of nanomaterials to enter the cell. In the present study, the particle size of 26.9 nm indicates that nanoparticles are small and toxic because of their preferable mobility inside the BBB (Osborne et al. 2013) wherein directly disturb BBB and could be easily transported by the trans-synaptic neurons. This is consistent with the previous studies that revealed 25-nm silver nanoparticles cause significant neurotoxicity both in vivo and in vitro (Rahman et al. 2008, 2009).

Regarding the accumulation of AgNPs in the present findings, the possible mechanism can be proposed as the sulfur molecules are rich in thiol groups and intent to bind with Ag substrates. The formation of new bonds leads to sulfur molecules tightly adsorbing on the surfaces of AgNPs particles. In this case, the chemical enhancements derived from AgNPs make up for the efficiency of the surface effect of Ag metals (Guo et al. 2019). Further, the disposition of AgNPs could be ascribed to the damage of cell integrity and increase in-stream opening the gates (Antsiferova et al. 2019). According to Wen et al. (2016), accumulation of AgNPs depends on its surface

oxidation to release silver nano ions. Zhang et al. (2011) suggested traversing the nanoparticles across the BBB through dissolving membranes of the endothelial cells. Unlike the present data, the high accumulation of brain silver may be surmised by the difference in size average (56 nm, 60 nm) and the variation in the value of doses (Kim et al. 2008, 2010). Therefore, size-dependent increases of silver accumulation in the brain indicate that the orally absorbed silver nanoparticles have the bioavailability to penetrate and distribute in the blood-brain circulation and the possible deposition that may be due to particle size as opposed to ionized silver. On the other hand, the high total brain contents of silver in the present study might be interpreted by the powerful affinity of nanoparticles to the thiol group of free brain sulfur and sulfur-linked proteins forming thiol-silver complex (Liu et al., 2010) which also may contribute to the explanation of the neurotoxic effects of nanosilver (Elle et al. 2013). This great affinity of silver to sulfur could also indicate the high merging of silver ions with sulfur-rich biological constituents (Loeschner et al. 2011).

A decrease of neurotransmitter concentrations was detected in AgNP-treated rats suggesting that the AgNP has a differential tight binding to neurotransmitters and more bracing architecture in which can be rapidly restrained in and out through the synapse trafficking (Varela et al. 2016). Besides, organic cation transporters (OCT) are facilitative transporters that are mediating the translocation of small organic cations across the basolateral membranes (Wagner et al. 2016). In the present findings, the significantly decreased choline, serotonin, and dopamine concentrations may be attributable to downregulation of protein and mRNA expression levels of the OCT, indicating that OCT is the target for silver nano. The present findings conflict Hadrup et al. (2012) who found an increase in the concentration of the dopamine in rat brain suggesting a differential effect of silver on dopamine relying on the length of exposure. According to findings in Parkinson's disease, the decreased brain dopamine concentrations following of AgNP administration could be explained by an increase in apoptosis of dopaminergic neurons (Savitt et al. 2006; Ehringer and Hornykiewicz 2012). Further, in vitro data suggest that AgNPs change the regulation of mRNA levels of dopamine-related expressed genes during neural cell differentiation (Wang et al., 2009a, b; Powers et al. 2010, 2011). Probably, this indicates distinct variations in the effects of silver nanoparticles on the regulation of neurotransmitter-related genes associated with normal brain activity. Crossing, distribution, and deposition of AgNPs in the presynaptic endings could provide another possible evidence of deficiency of neurotransmitters (Fedorovich et al. 2010; Tang et al. 2010). Also, the deficit neurotransmitters may suggest axonal defects (dysplasia) due to mutation in gene expression of Growth Associated Protein 43 (GAP43) that critical motif of the axon and synaptic terminals (Rosskothen-Kuhl and Robert-Benjamin 2014; Liu et al., 2020a, b).

In the present study, the brain acetylcholinesterase (AChE) activity significantly declined in both low and high doses indicating that AgNPs cause nervous toxicity (Bugata et al. 2019). However, the precise mechanism identifying that the AgNPs inhibit cholinesterase activities is still not understood in relating to interactions between nanoparticles and enzyme. It has been suggested that adsorption of the AChE on AgNPs surface and the subsequent embracing of enzyme configuration is the primary mechanism influenced by the distribution of surface charges on an enzyme (Wang et al., 2009a, b; Šinko et al. 2014). There is evidence that impairment of brain serotonin (5-HT) may be prompted by the sustained extreme attrition of tryptophan (Neumeister et al. 2002). ElMazoudy et al. (2015, 2020) reported that severe tryptophan depletion could lead to degradation of neural 5-HT levels suggesting the tight binding of tryptophan to the surface of nanoparticles (Hernández et al. 2018). As silver nanoparticles possess superior biophysical properties with regard to electrical conductivity and relative permittivity (Khan et al. 2011), so, the decrease of neurotransmitters that are parallel with the decrease in electrical conductivity and dielectric permittivity of the brain refers to a deficit in brain circuitry.

The decreased electrical conductivity and relative permittivity in the present results may be attributed to the disturbances in dipoles of nanosilver relating to the field direction of the brain (Zhang et al. 2010). The electron-trapping and molecular ionization of nanofluid mechanisms may be also implicated in the reduction of electrical conductivity and relative permittivity (cerebrospinal fluid) (Prasad et al. 2006; Fal et al. 2016). Additional studies showed that reduced conductivity and relative permittivity may be attributable to the morphological defects in myelin sheaths and mutation in the gene expression of myelin glycoproteins suggesting that the nerve fibers (myelinated) may be a target of AgNPs (Dabrowska-Bouta et al. 2019). Furthermore, Schmid and Überbacher (2005) and Peyman (2011) concluded that impaired myelination observed in the present findings may be the cause of the decline in the values of permittivity and conductivity.

Neurotoxicity induced via high oxidative stress in the present study is assigned to the stimulation of downregulation of CAMKII (CAMK2A/CAMK2B) protein expression, which results in synapse deformation, apoptosis, and perturbation of signal transduction and the demise of axons and neural dendrites (Chen et al. 2011; Mockett et al. 2011; Hamdani et al. 2013). These pathways suggest that nanosilver might be closely implicated and extremely mediate molecular signalling of the synaptic development and morphogenesis through the calcium/calmodulin-regulated kinase mechanisms. Besides, the oxidative stress damages dopaminergic neurons via excessive releasing of pro-inflammatory cytokines (IL-1β, IL-6, IL-8, TNF-α) and their inflammatory mediators (nitric oxide synthase and cyclooxygenase-2) and that explains the decrease in dopamine activity in the present

findings (Malú and Matthew 2010; Joshi and Singh 2018). Thereby, the damage of dopaminergic nerve cells and abnormal signal transduction activating further neuroglia are essential tools for identifying mechanisms of neurodegenerative diseases and potential treatments. Meanwhile, the damage of dopaminergic regulation of neurons may attribute to influence and permanent oxidative stress that probably provoke inflammation-related transcription factors (Tarique et al. 2016). The caspase3 enzyme is another oxidative stress-mediator factor essential for the apoptotic death in diverse neurodegenerative diseases through regulation of endogenous mechanisms implicated in the caspase3-dependent apoptosis transcription factors referring to a critical role of AgNPs in the normal regulation of neuronal apoptosis in vivo (Nijhawan et al. 2000; Bazan-Peregrino et al. 2007; Yin et al., 2013a, b).

In the present findings, the deficiency of the neurotransmitters could reflect the inefficiency of nerve fibers as transmission pathways which may due to damage to the neuronal cytoskeleton, shortening of nerve fibers, or reduction in the number of nerve nodes (axon diameter) induced by damage of neurofilament protein-H (NF-H), tubulin-α, or tubulin-β, causing obstruction of the axonal transport and nerve conduction velocity (Ayaz et al. 2012; Kengaku 2018; Liu et al., 2020a, b). Therefore, the suppressed dopamine, acetylcholine, and serotonin in present findings could be a local injury induced by AgNPs on nerve fibers (Wang et al. 2003). In this context, inhibition of neurotransmitters in vivo is dependent on the brain electric conductivity and dielectric permittivity. So, the present results provide many conclusions related to perceive the intended mechanism of how the brain can regulate the physicochemical conditions to control signal transductions in real time. On the other hand, Michel et al. (2017) reported that the alterations of brain biophysical properties reflect brain toxicity and indicate a disturbance of brain water contents causing tissue necrosis, tissue abscess, and tissue cysts. Further, decreased brain conductivity may be attributed to median impedances of gray and white matter cerebral tissues wherein gray matter shows lower median impedances in neurodegenerative diseases (Koessler et al. 2017).

Conclusions

From the present findings, we can surmise that profilings of disruption in brain electric conductivity and dielectric permittivity, oxidative stress, deficiency in brain neurotransmitters, and robust damage of myelinated nerve fibers firmly proved the neurotoxic hazards of AgNPs. The results also revealed the existence of robust toxicity of AgNPs at 100- and 1000-mg/kg dose levels and particle size 29.6 nm indicating the probable capability of crossing-over the BBB. The deposition of silver in brain organ was higher in the AgNP-treated groups than in the control rats indicating the ionic bioavailability of silver rather than nanoparticles. Finally, present findings suggest the deficit of neurotransmitters may be via axonal and dendrites defects and/or disruption in neurotransmitter-transporter gene expression as well as brain circuitry that raise a serious explanation of brain toxicity like aging, Parkinson's disease, and Alzheimer's disease. Therefore, the electric conductivity and dielectric permittivity profiling may be helpful in layout brain toxicity studies as indications on the dynamics and kinetics in brain tissues and could provide decisive information and comprehension by determining signal transduction levels in potential neurodegeneration for exposure aspects.

Abbreviations *AChE,* Acetylcholine esterase; *BBB,* Blood-brain barrier; *DA,* Dopamine; *EDX,* Energy-dispersive X-ray; *NPs,* Nanoparticles; *ROS,* Reactive oxygen species; *TEM,* Transmission electron microscope

Availability of data and materials Not applicable.

Author contribution Azza Attia, Heba Ramadan: conceptualization, methodology, software. Azza Attia: photomicrographs (light and electron microscopy). Azza Attia, Heba Ramadan, Asmaa Abdelnaser: data curation. Reda ElMazoudy: writing—original draft preparation. Azza Attia, Reda ElMazoudy: visualization, investigation, writing—reviewing and editing.

Declarations

Ethical approval Experimental procedures were achieved in conformation with principles of laboratory animal care and approved by the Institutional Animal Care and Use Committee (IACUC) Alexandria University, Alexandria (Registration no: AU 04-19-10-21-3).

Consent to publish Not applicable.

Competing interests The authors declare that they have no competing interests.

References

Adeyemi OS, Adewumi I (2014) Biochemical evaluation of silver nanoparticles in Wistar rats. Int Schol Res Notices 2014 Article ID 196091: 8 pages.

Anton AH, Sayre DF (1964) The distribution of dopamine and dopa in various animals and a method for their determination in diverse biological materials. J Pharmac exp Ther 145:326–336

Antsiferova AA, Kopaeva MY, Kochkin VN, Kashkarov PK, Kovalchuk MV (2019) Accumulation of silver nanoparticles in mice brain parts and the harmful effects. J Nanomed Nanotechnol 10(1):524

Ayaz P, Ye X, Huddleston P, Brautigam CA, Rice LM (2012) A TOG: αβ-tubulin complex structure reveals conformation-based mechanisms for a microtubule polymerase. Science 337(6069):857–860

Azocar MI, Alarcon R, Castillo A, Blamey JM, Walter M, Paez M (2019) Capping of silver nanoparticles by anti-inflammatory ligands: antibacterial activity and superoxide anion generation. J Photochem Photobiol B 193:100–108

Bancroft JD, Gamble M, (2008) Theory and practice of histological techniques. Churchill Livingstone Elsevier, Philadelphia, PA

Baruwati B, Steven O, Simmons M, Rajendar S, Bellina V (2013) "Green" synthesized and coated nanosilver alters the membrane permeability of barrier (intestinal, brain endothelial) cells and stimulates oxidative stress pathways in neurons. ACS Sustain Chem Eng 1(7):753–759

Bazan-Peregrino M, Gutierrez-Kobeh L, Moran J (2007) Role of brain-derived neurotrophic factor in the protective action of N-methyl-D-aspartate in the apoptotic death of cerebellar granule neurons induced by low potassium. J Neurosci Res 85:332–341

Blaser SA, Sheringer M, Macleod M, Hungerbuhler K (2008) Estimation of cumulative aquatic exposure and risk due to silver: contribution of nanofunctionalized plastics and textiles. Sci Total Environ 390:396–409

Bugata LSP, Venkata PP, Gundu AR, Fazlur RM, Reddy UA, Kumar JM, Mekala VR, Bojja S, Mahboob M (2019) Acute and subacute oral toxicity of copper oxide nanoparticles in female albino Wistar rats. J Appl Toxicol 39:702–716

Chen S, Xu Y, Xu B, Guo M, Zhang Z, Liu L, Chen L (2011) CaMKII is involved in cadmium activation of MAPK and mTOR pathways leading to neuronal cell death. J Neurochem 119:1108–1118

Choi O, Hu Z (2008) Size dependent and reactive oxygen species related nanosilver toxicity to nitrifying bacteria. Environ Sci Technol 42(12):4583–4588

Cupaioli FA, Zucca FA, Boraschi D, Zecca L (2014) Engineered nanoparticles. How brain friendly is this new guest? Prog Neurobiol 119-120:20–38

Dabrowska-Bouta B, Sulkowski G, Strużyński W, Strużyńska L (2019) Prolonged exposure to silver nanoparticles results in oxidative stress in cerebral myelin. Neurotox Res 35(3):495–504

Ehringer H, Hornykiewicz O (2012) Distribution of noradrenaline and dopamine (3-hydroxytyramine) in the human brain and their behavior in diseases of the extrapyramidal system. Klin Wochenschr 38: 1236–1239

Elle RE, Gaillet S, Vide J, Romain C, Lauret C, Rugani N, Cristol JP, Rouanet JM (2013) Dietary exposure to silver nanoparticles in Sprague-Dawley rats: effects on oxidative stress and inflammation. Food Chem Toxicol 60:297–301

Ellman GL, Courtney KD, Andres V, Featherstone RM (1961) A new and rapid colorimetric determination of acetylcholinesterase activity. Biochem Pharmacol 7(2):88–95

ElMazoudy R, AbdelHameed N, ElMasry A (2015) Paternal dapoxetine administration induced deterioration in reproductive performance, fetal outcome, sexual behavior, biochemistry of male rats. Int J Impot Res 27:206–214

ElMazoudy R, El-Abd K, Mekkawy D, Kameld K (2020) Developmental effects on hypothalamic, hypophyseal, testicular and steroidogenic patterns of sertraline-exposed male rats by accumulated doses from juvenile to puberty. Ecotoxicol Environ Saf 188:109840

Eom HJ, Ahn JM, Kim Y, Choi J (2013) Hypoxia inducible factor-1 (HIF-1)-flavin containing monooxygenase-2 (FMO-2) signaling acts in silver nanoparticles and silver ion toxicity in the nematode. Toxicol Appl Pharmacol 270:106–113

Fal J, Barylyak A, Besaha K, Bobitski YV, Cholewa M, Zawlik I, Szmuc K, Cebulski J, Zyła G (2016) Experimental investigation of electrical conductivity and permittivity of SC-TiO2-EG. Nanofluids. Nanoscale Res Lett 11:375–394

Fedorovich SV, Alekseenko AV, Waseem TV (2010) Are synapses targets of nanoparticles? Biochem Soc Trans 38(2):536–538

Genter MB, Newman NC, Shertzer HG, Ali SF, Bolon B (2012) Distribution and systemic effects of intranasally administered 25 nm silver nanoparticles in adult mice Toxicol. Pathol. 40:1004

Grosse S, Evje L, Syversen T (2013) Silver nanoparticle-induced cytotoxicity in rat brain endothelial cell culture. Toxicol In Vitro 27:305–313

Guo J, Liu G, Ma Q, Yang S, Li Y, Cai W (2019) Fabrication of Ag-nanosheets-built micro/nanostructured arrays via *in situ* conversion on Cu_2O-coated Si nanocone platform and their highly structurally enhanced SERS effect. Nanotechnol 30(34):345302

Hadrup N, Loeschner K, Mortensen A, Sharma AK, Qvortrup K, Larsen EH, Lam HR (2012) The similar neurotoxic effects of nanoparticulate and ionic silver in vivo and in vitro. Neurotoxicol 33:416–423

Hamdani N, Krysiak J, Kreusser MM, Neef S, dos Remedios CG, Maier LS, Linke WA (2013) Crucial role for Ca2+/calmodulin-dependent protein kinase-II in regulating diastolic stress of normal and failing hearts via titin phosphorylation. Circ Res 112:664–674

Hernández B, Tinacci L, Coïc Y-M, Chenal A, Cohen R, Sanchez-Cortes S, Ghomi M (2018) Tryptophan tight binding to gold nanoparticles induces drastic changes in indole ring Raman markers. J Phys Chem C 122(24):13034–13046

Huang CL, Hsiao L, Chen HL, Wang CF, Huang Y, Chuang C (2015) Silver nanoparticles effect on gene expression of inflammatory and neurodegenerative responses in mouse brain neural cells. Environ Res 136:253–263

Hussain SM, Javorina AK, Schrand AM, Duhart HM, Ali SF, Schlager JJ (2006) The interaction of manganese nanoparticles with PC-12 cells induces dopamine depletion. Toxicol Sci 92:456–463

Iqbal S, Du XJ, Wang JL, Li HJ, Yuan YY, Wang J (2018) Surface charge tunable nanoparticles for TNF-α siRNA oral delivery for treating ulcerative colitis. Nano Res 11(5):2872–2884

Islam MA, Barua S, Barua D (2017) A multiscale modeling study of particle size effects on the tissue penetration efficacy of drug-delivery nanoparticles. BMC Syst Biol 11(1):113

Joshi N, Singh S (2018) Updates on immunity and inflammation in Parkinson disease pathology. J Neurosci Res 96(3):379–390

Kabir MT, Sahab Uddin M, Zaman S, Begum Y, Ashraf Md G, Bin-Jumah MN, Bungau SG, Mousa SA, Abdel-Daim MM (2021) Molecular mechanisms of metal toxicity in the pathogenesis of Alzheimer's disease. Mol Neurobiol 58:1–20

Kengaku M (2018) Cytoskeletal control of nuclear migration in neurons and non-neuronal cells. Proc Jpn Acad Ser B 94:337–349

Khan MAM, Kumar S, Ahamed M, Alrokayan SA, AlSalhi MS (2011) Structural and thermal studies of silver nanoparticles and electrical transport study of their thin films. Nanoscale Res Lett 6(1):434. https://doi.org/10.1186/1556-276x-6-434.

Kim YS, Kim JS, Cho HS, Rha DS, Kim JM (2008) Twenty-eight-day oral toxicity, genotoxicity, and gender-related tissue distribution of silver nanoparticles in Sprague-Dawley rats. Inhal Toxicol 20:575–583

Kim YS, Song MY, Park JD, Song KS, Ryu HR, Chung YH, Chang HK, Lee JH, Oh KH, Kelman BJ, Hwang IK, Yu IJ (2010) Subchronic oral toxicity of silver nanoparticles. Part Fibre Toxicol 7:20

Koessler L, Colnat-Coulbois S, Cecchin T, Hofmanis J, Dmochowski JP, Norcia AM, Maillard LG (2017) In-vivo measurements of human brain tissue conductivity using focal electrical current injection through intracerebral multicontact electrodes. Hum Brain Mapp 38:974–986

Koracevic D, Koracevic G, Djordjevic V, Andrejevic S, Cosic V (2001) Method for the measurement of antioxidant activity in human fluids. J Clin Pathol 54(5):356–361

Lee GS, Simpson C, Sun B-H, Yao C, Foer D, Sullivan B, Matthes S, Alenina N, Belsky J, Bader M, Insogna KL (2014) Measurement of plasma, serum, and platelet serotonin in individuals with high bone mass and mutations in LRP5. J Bone Miner Res 29(4):976–981

Lin DH, Xing BS (2007) Phytotoxicity of nanoparticles: inhibition of seed germination and root growth. Environ Pollut 150:243–250

Liu J, Sonshine DA, Shervani S, Hurt RH (2010) Controlled release of biologically active silver from nanosilver surfaces. ACS Nano 4: 6903–6913

Liu Y, Guan W, Ren G, Yang Z (2012) The possible mechanism of silver nanoparticle impact on hippocampal synaptic plasticity and spatial cognition in rats. Toxicol Lett 209:227–231

Liu H, Yang H, Fang Y, Li K, Tian L, Liu X, Zhang W, Tan Y, Lai W, Bian L, Lin B, Xi Z (2020a) Neurotoxicity and biomarkers of zinc oxide nanoparticles in main functional brain regions and dopaminergic neurons. Sci Total Environ 705:135809

Liu Y, Sun L, Yang G, Yang Z (2020b) Nephrotoxicity and genotoxicity of silver nanoparticles in juvenile rats and possible mechanisms of action. Arch Ind Hyg Toxicol 71:121–129

Loeschner K, Hadrup N, Qvortrup K, Larsen A, Gao X, Vogel U, Mortensen A, Lam HR, Larsen EH (2011) Distribution of silver in rats following 28 days of repeated oral exposure to silver nanoparticles or silver acetate. Part Fibre Toxicol 8:18

Malú GT, Matthew SG (2010) Neuroinflammation in Parkinson's disease: its role in neuronal death and implications for therapeutic intervention. Neurobiol Dis 37(3):510–518

Maneewattanapinyo P, Banlunara W, Thammacharoen C, Ekgasit S, Kaewamatawong T (2011) An evaluation of acute toxicity of colloidal silver nanoparticles. J Vet Med Sci 73(11):1417–1423

Medina C, Santos-Martinez MJ, Radomski A, Corigan OI, Radomski MW (2007) Nanoparticles: pharmacological and toxicological significance. Br J Pharmacol 150:552–558

Michel E, Hernandez D, Lee SY (2017) Electrical conductivity and permittivity maps of brain tissues derived from water content based on T1-weighted acquisition. Mag Reason Med 77:1094–1103

Mockett BG, Guévremont D, Wutte M, Hulme SR, Williams JM, Abraham WC (2011) Calcium/calmodulin-dependent protein kinase II mediates group I metabotropic glutamate receptor-dependent protein synthesis and long-term depression in rat hippocampus. J Neurosci 31:7380–7391

Neumeister A, Konstantinidis A, Stastny J, Schwarz MJ, Vitouch O, Willeit M, Praschak-Rieder N, Zach J, Zwaan M, Bondy B, Ackenheil M, Kasper S (2002) Association between serotonin transporter gene promoter polymorphism (5HTTLPR) and behavioral responses to tryptophan depletion in healthy women with and without family history of depression. Arch Gen Psychiatry 59:613–620

Nijhawan D, Hornarpour N, Wang X (2000) Apoptosis in neural development and disease. Annu Rev Neurosci 23:73–87

Osborne OJ, Johnston B, Moger J, Baalousha M, Lead J, Kudoh T, Tyler C (2013) Effects of particle size and coating on nanoscale Ag and TiO2 exposure in zebrafish (Danio rerio) embryos. Nanotoxicol 7: 1315–1324

Pal S, Tak YK, Joon Myong Song JM (2007) Does the antibacterial activity of silver nanoparticles depend on the shape of the nanoparticle? A study of the Gram-negative bacterium *Escherichia coli*. Appl Environ Microbiol 3(6):1712–1720

Park EJ, Yi J, Kim Y, Choi K, Park K (2010) Silver nanoparticles induce cytotoxicity by a Trojan-horse type mechanism. Toxicol in Vitro 24(3):872–878

Peyman A (2011) Dielectric properties of tissues; variation with age and their relevance in exposure of children to electromagnetic fields; state of knowledge. Prog Biophys Mol Biol 107:434–438

Powers CM, Wrench N, Ryde IT, Smith AM, Seidler FJ, Slotkin TA (2010) Silver impairs neurodevelopment: studies in PC12 cells. Environ Health Perspect 118:73–79

Powers CM, Badireddy AR, Ryde IT, Seidler FJ, Slotkin TA (2011) Silver nanoparticles compromise neurodevelopment in PC12 cells: critical contributions of silver ion, particle size, coating, and composition. Environ Health Perspect 119:37–44

Prasad SK, Sandhya KL, Nair GG, Hiremath US, Yelamaggad CV, Sampath S (2006) Electrical conductivity and dielectric constant measurements of liquid crystal–gold nanoparticle composites. Liq Cryst 33(10):1121–1125

Pröfrock D, Prange A (2012) Inductively coupled plasma–mass spectrometry (ICP-MS) for quantitative analysis in environmental and life sciences: a review of challenges, solutions, and trends. App Spectroscopy 66(8):843–868

Rahman MF, Wang J, Patterson TA, Duhart HM, Newport GD, Hussain SM, Schlager JJ, Ali SF, (2008) Neurotoxicity assessment of sliver-25 nanoparticles: an in vitro and in vivo study. Toxicol. CD official J. Soc. Toxicol. 102(S-1)

Rahman MF, Wang J, Patterson TA, Saini UT, Robinson BL, Newport GD, Murdock RC, Schlager JJ, Hussain SM, Ali SF (2009) Expression of genes related to oxidative stress in the mouse brain after exposure to silver-25 nanoparticles. Toxicol Lett 187:15–21

Robards AW, Wilson AJ, (1993) Procedures in electron microscopy, John Wiley & Sonns Ltd, Chichester. New York. Brisbane. Toronto. Singapore

Rosskothen-Kuhl N, Robert-Benjamin I (2014) G*ap43* transcription modulation in the adult brain depends on sensory activity and synaptic cooperation. PLoS One 9(3):e92624

Ryu JK, Shin WH, Kim J, Joe EH, Lee YB, Cho KG, Oh YJ, Kim SU, Jin BK (2002) Trisialoganglioside GT1b induces in vivo degeneration of nigral dopaminergic neurons: role of microglia. Glia 38:15–23

Sahab Uddin Md, Rashid M (2020) Advances in neuropharmacology: drugs and therapeutics/edited by Md. Sahab Uddin and Mamunur Rashid (Editors) Apple Academic Press Inc. ISBN 9781771887977

Sahab Uddin M, Al Mamun A, Md TK, Ahmad J, Jeandet P, Md SS, Ashraf GM, Aleya L (2020a) Neuroprotective role of polyphenols against oxidative stress-mediated neurodegeneration. Eur J Pharmacol 886:173412

Sahab Uddin M, Kabir Md T, Al Mamun A, Barreto GE, Rashid M, Perveen A, GMd A (2020b) Pharmacological approaches to mitigate neuroinflammation in Alzheimer's. Dis Int Immunopharmacol 84: 106479

Sahab Uddin M, Kabir Md T, Al Mamun A, Behl T, Mansouri RA, Aloqbi AA, Perveen A, Hafeez A, Ashraf GM (2021) Exploring potential of alkaloidal phytochemicals targeting neuroinflammatory signaling of Alzheimer's. Curr Pharm Des 27(3):357–366

Savitt JM, Dawson VL, Dawson TM (2006) Diagnosis and treatment of Parkinson disease: molecules to medicine. J Clin Invest 116:1744–1754

Schmid G, Überbacher R (2005) Age dependence of dielectric properties of bovine brain and ocular tissues in the frequency range of 400 MHz to 18 GHz. Phys Med Biol 50:4711–4720

Schrand AM, Rahman MF, Hussain SM, Schlager JJ, Smith DA, Syed AF (2010) Metal-based nanoparticles and their toxicity assessment. Nanomed Nanobi 2:544–568

Sharma HS, Hussain S, Schlager J, Ali SF, Sharma A (2010) Influence of nanoparticles on blood-brain barrier permeability and brain edema formation in rats. Acta Neurochir Suppl 106:359–364

Šinko G, Vrček IV, Goessler W, Leitinger G, Dijanošić A, Miljanić S (2014) Alteration of cholinesterase activity as possible mechanism of silver nanoparticle toxicity. Environ Sci Pollut Res 21:1391–1400

Stasiuk M, Bartosiewicz D, Kozubek A (2008) Inhibitory effect of some natural and semisynthetic phenolic lipids upon acetylcholinesterase activity. Food Chem 108:996–1001

Struzynski W, Dabrowska-Bouta B, Grygorowicz T, Zieminska E, Struzynska L (2014) Markers of oxidative stress in hepatopancreas of crayfish (Orconecteslimosus, raf.) experimentally exposed to nanosilver. Environ Toxicol 29:1283–1291

Tang J, Xiong L (2009) Distribution, translocation and accumulation of silver nanoparticles in rats. J Nanosci Nanotechnol 9(8):4924–4932

Tang J, Xiong L, Wang S, Wang J, Liu L, Li J, Wan Z, Xi T (2008) Influence of silver nanoparticles on neurons and blood–brain barrier via subcutaneous injection in rats. Appl Surf Sci 255:502–504

Tang J, Xiong L, Zhou G, Wang S, Wang J, Liu L, Li J, Yuan F, Lu S, Wan Z, Chou L, Xi T (2010) Silver nanoparticles crossing through and distribution in the blood–brain barrier in vitro. J Nanosci Nanotechnol 10:6313–6317

Tarique H, Bie T, Yulong Y, Francois B, Myrlene CBT, Najma R (2016) Oxidative stress and inflammation: what polyphenols can do for us? Oxidative Med Cell Longev 2016:1–9

Trickler WJ, Lantz SM, Murdock RC, Schrand AM, Robinson BL, Newport GD, Schlager JJ, Oldenburg SJ, Paule MG, Slikker W Jr, Hussain SM, Ali SF (2010) Silver nanoparticle induced blood–brain barrier inflammation and increased permeability in primary rat brain microvessel endothelial cells. Toxicol Sci 118:160–170

Varela JA, Dupuis JP, Etchepare L, Espana A, Cognet L, Groc L (2016) Targeting neurotransmitter receptors with nanoparticles in vivo allows single-molecule tracking in acute brain slices. Nat Commun 7: 10947

Wagner DJ, Hu T, Wang J (2016) Polyspecific organic cation transporters and their impact on drug intracellular levels and pharmacodynamics. Pharmacol Res 111:237–246

Wang H, Yu M, Ochani M, Amella CA, Tanovic M, Susarla S, Li JH, Wang H, Yang H, Ulloa L, Al-Abed Y, CJ C, Tracey KJ (2003) Nicotinic acetylcholine receptor α7 subunit is an essential regulator of inflammation. Nature 421:384–388

Wang J, Rahman MF, Duhart HM, Newport GD, Patterson TA, Murdock RC, Hussain SM, Schlager JJ, Ali SF (2009a) Expression changes of dopaminergic system-related genes in PC12 cells induced by manganese, silver, or copper nanoparticles. Neurotoxicol. 30:926–933

Wang Z, Zhao J, Li F, Gao D, Xing B (2009b) Adsorption and inhibition of acetylcholinesterase by different nanoparticles. Chemosphere 77: 67–73

Wang CI, Chen WT, Chang HT (2012) Enzyme mimics of Au/Ag nanoparticles for fluorescent detection of acetylcholine. Anal Chem 84: 9701–9706

Wang Z, Xia T, Liu S (2015) Mechanisms of nanosilver-induced toxicological effects: more attention should be paid to its sublethal effects. Nanoscale. 7(17):7470–7481

Wegner C, Esiri MM, Chance SA, Palace J, Matthews PM (2006) Neocortical neuronal, synaptic, and glial loss in multiple sclerosis. Neurology 67:960–977

Wen R, Yang X, Hu L, Sun C, Zhou Q, Jiang G (2016) Brain-targeted distribution, and high retention of silver by chronic intranasal instillation of silver nanoparticles and ions in Sprague-Dawley rats. J Appl Toxicol 36:445–453

Xu F, Piett C, Farkas S, Qazzaz M, Syed NI (2013) Silver nanoparticles (AgNPs) cause degeneration of cytoskeleton and disrupt synaptic machinery of cultured cortical neurons. Mol Brain 6:29

Xu L, Shao A, Zhao Y, Wang Z, Zhang C, Sun Y, Deng J, Chou LL (2015) Neurotoxicity of silver nanoparticles in rat brain after intragastric exposure. J Nanosci Nanotechnol 15:4215–4223

Yin N, Liu Q, Liu J, He B, Cui L, Li Z, Yun Z, Qu G, Liu S, Zhou Q, Jiang G (2013a) Silver nanoparticle exposure attenuates the viability of rat cerebellum granule cells through apoptosis coupled to oxidative stress. Small 9(9-10):1831–1841

Yin N, Liu Q, Liu J, He B, Cui L, Li Z (2013b) Silver nanoparticle exposure attenuates the viability of rat cerebellum granule cells through apoptosis coupled to oxidative stress. Small 9:1831–1841

Zahin N, Anwar R, Tewari D, Kabir T, Sajid A, Mathew B, Uddin S, Aleya L, Abdel-Daim MM (2020) Nanoparticles and its biomedical applications in health and diseases: special focus on drug delivery. Environ Sci Pollut Res 27:19151–19168

Zhang D, Chava S, Berven C, Lee SK, Devitt R, Katkanant V (2010) Experimental study of electrical properties of ZnO nanowire random networks for gas sensing and electronic devices. Appl Phys A Mater Sci Process 100(1):145–150

Zhang W, Yao Y, Sullivan N, Chen YS (2011) Modeling the primary size effects of citrate-coated silver nanoparticles on their ion release kinetics. Environ Sci Technol 45:4422–4428